Hydrol. Earth Syst. Sci. Discuss., 9, 9043–9064, 2012
www.hydrol-earth-syst-sci-discuss.net/9/9043/2012/
doi:10.5194/hessd-9-9043-2012

Hydrology and Earth System Sciences Discussions

Mapping spatially-temporally continuous shortwave albedo for global land surface from MODIS data

N. Liu[1], Q. Liu[1,2,*], L. Wang[3], S. Liang[2,4], J. Wen[1], Y. Qu[3], and S. Liu[3]

[1]State Key Laboratory of Remote Sensing Science, Jointly Sponsored by Institute of Remote Sensing Applications, Chinese Academy of Sciences and Beijing Normal University, Beijing, China
[2]College of Global Change and Earth System Science, Beijing Normal University, Beijing, China
[3]School of Geography, Beijing Normal University, Beijing, China
[4]Department of Geography, University of Maryland, College Park, Maryland, USA
[*]now at: Institute of Remote Sensing Applications, Chinese Academy of Sciences, Beijing, China

Received: 6 July 2012 – Accepted: 15 July 2012 – Published: 30 July 2012

Correspondence to: Q. Liu (liuqiang@irsa.ac.cn)

Published by Copernicus Publications on behalf of the European Geosciences Union.

Abstract

Land-surface albedo plays a critical role in the Earth's radiant energy budget studies. Satellite remote sensing is an effective approach to acquire regional and global albedo observations. However, owing to cloud coverage, seasonal snow and sensor malfunctions, spatially-temporally continuous albedo datasets are often inaccessible. GLASS preliminary albedo datasets (GLASS02A2x, $x = 1$, 2, 3 and 4) are newly developed global daily land-surface albedo products. Like other products, GLASS02A2x albedo surfers from large areas of missing data. Beside this, sharp fluctuations exist in GLASS02A2x time series due to data noise and algorithm uncertainties. In this study, a statistics-based temporal filterer (STF) is proposed to fill the data gaps and smooth the fluctuations in GLASS02A2x albedo time series. The result of STF algorithm is the GLASS final albedo product (GLASS02A06). Results show that the STF method has greatly improved the integrity and smoothness of the GLASS final albedo product. Seasonal trends in albedo are well depicted by the GLASS final albedo product. Compared with MODIS product, the final GLASS albedo product is much more competent in capturing the surface albedo variations. Although the STF algorithm is designed for GLASS albedo product, it is able to incorporate other albedo products. The STF method may also be applied to other parameters, such as the LAI and soil moisture.

1 Introduction

Land-surface albedo refers to the ratio of reflected to incoming solar radiation at the Earth's surface over the solar spectral domain (Dickinson, 1983). As one of the fundamental forcing parameters in climate models, surface albedo plays an important role in the Earth's radiant energy budget (Barnes and Roy, 2008,2010; Liang et al.,2010; Manalo-Smith et al., 1998). Spatial-temporal variability in albedo is often associated with environmental change and human activities as well (Bsaibes et al., 2009; Dirmeyer and Shukla, 1994; Jin and Roy, 2005; Moritz et al., 2002). According to the Global

HESSD
9, 9043–9064, 2012

Climate Observing System (GCOS), spatially-temporally continuous albedo products with a relative accuracy of 5 %, 1-km spatial resolution and 1-day temporal resolution are required by climatic studies (GCOS, 2006). However, several factors such as cloud coverage, seasonal snow cover and sensor malfunction, lead to large areas of data gaps in current albedo products. Take the Moderate Resolution Imaging Spectroradiometer (MODIS) standard albedo product (MCD43B3) as an example, about 20 to 40 % of the global land pixels miss valid shortwave black-sky albedo every year (Table 1).

A variety of strategies have been proposed to enhance the completeness of current albedo datasets. One approach is to improve the inputs to the retrieving algorithm. Based on the standard retrieving technique of MODIS nadir BRDF-adjusted (NBAR) reflectance products, an adapted method was employed to improve the integrity of reflectance series (Ju et al., 2010). A Kalman filter was used to improve the completeness of BRDF coefficients series (Samain et al., 2008). Beside the above mentioned strategy, post-processing based on the current albedo products is another solution for filling albedo gaps. An ecosystem curving fitting (ECF) method was performed on MOD43B3 product to generate spatially complete albedo datasets (Moody et al., 2005). In the context of ECF method, missing data are interpolated by using pixel-level and regional albedo climatology curves. However, Fang et al.'s (2007, 2008) studies demonstrated that multiyear average is more suitable than regional average for characterizing a pixel's profile. Fang et al. (2007, 2008) designed a temporal-spatial filter (TSF) to generate gapless albedo and leaf area index (LAI) products. In TSF method, multiyear averages at each pixel are first determined from multiyear observations. Then, both multiyear averages and neighboring observations are averaged with weights to replace missing values.

The objective of this study is to map spatially-temporally continuous daily shortwave albedo for global land surface. The paper is organized as follows: Sect. 2 introduces the GLASS preliminary albedo products. A statistics-based temporal filterer is described in Sect. 3. Section 4 analyzes the results and Sect. 5 concludes this study.

HESSD
9, 9043–9064, 2012

2 GLASS preliminary albedo products

Global land surface satellite (GLASS) is a project sponsored by Chinese "State Program for High-Tech Research and Development" program, which aims at providing a suite of key land surface parameter datasets with high quality for global change and climatic study. GLASS albedo is generated in two steps. In the first step, albedo is retrieved from remote sensing data by the inversion of radiative transfer process, or its simplification. The resultant albedo retrieved in the first step is called GLASS preliminary product. In the second step, different kinds of preliminary products are post-processed into intermediate and final products. The GLASS preliminary albedo products are composed of four kinds of global daily 1km albedo datasets derived from two different inversion algorithms (Angular Bin, AB1 and AB2) and two kinds of reflectance inputs (MOD/MYD09GA and MOD/MYD02). The GLASS preliminary albedo products are named as GLASS02A2x, where $x = 1$ is for AB1 + MOD09GA combination, 2 is AB1 + MYD09GA, 3 is for AB2 + MOD02 and 4 is for AB2 + MYD02. Based on Liang's method, AB technique establishes a regression model that links spectral directional reflectance to shortwave albedo (Liang, 2003; Liang et al., 2005; Qu et al., 2012). The outputs of AB algorithm are shortwave black-sky albedo (BSA) at local solar noon, shortwave white-sky albedo (WSA) and quality assessment flag. The uncertainty information of AB retrievals is stored in quality assessment flag. Based on the GLASS preliminary products, the GLASS intermediate albedo products GLASS02A0x are obtained by averaging the good-quality GLASS02A2x albedo in 16 day temporal window on an 8-day cycle. Details of the GLASS preliminary and mediate albedo products are listed in Table 2.

The combination of AB algorithm and MODIS data has greatly improved the temporal resolution of GLASS preliminary products. However, there're still limitations in GLASS preliminary albedo products (Liu et al., 2011). First, GLASS02A2x albedo products suffer from frequent data gaps which are mainly caused by cloud coverage and seasonal snow. Second, GLASS02A2x albedo series fluctuate sharply because of data noises

HESSD
9, 9043–9064, 2012

and algorithm uncertainties. Finally, four GLASS preliminary albedo products need to be merged into one albedo product for the convenience of data users. In this paper, a statistics-based temporal filter (STF) is designed to post-process GLASS preliminary albedo products to generate spatially-temporally gapless albedo datasets.

3 Methodology

As illustrated in Fig. 1, the procedure of our STF algorithm comprises three parts. First, the a priori statistics of global surface albedo is calculated. Then, filter parameters are derived from the a priori statistics. Finally, the GLASS final product is generated by merging and filtering the four kinds of GLASS preliminary albedo products.

3.1 Statistics-based temporal filtering formula

Based on the temporal correlation of albedo measurements in neighboring days, it is reasonable to assume that the true albedo α_k on the k-th day is linearly correlated with the true albedo $\alpha_{k+\Delta k}$ on the $(k+\Delta k)$-th day:

$$\alpha_k = a_{\Delta k}\alpha_{k+\Delta k} + b_{\Delta k} \quad (1)$$

where both $a_{\Delta k}$ and $b_{\Delta k}$ are regression model coefficients. The model error $e_{\Delta k}$ is assumed to be Gaussian distributed with a zero mean and a $\zeta_{\Delta k}$ standard deviation (see Sect. 3.2 for the calculation of $a_{\Delta k}$, $b_{\Delta k}$ and $\zeta_{\Delta k}$). Then given the GLASS02A2x retrieval $\alpha^*_{k+\Delta k}$ and its uncertainty $\eta_{k+\Delta k}$ on the $(k+\Delta k)$-th day, the probability density function (PDF) of the true albedo α_k on the k-th day is in the form:

$$P\left(\alpha_k|\alpha^*_{k+\Delta k}\right) \sim N\left(a_{\Delta k}\alpha^*_{k+\Delta k} + b_{\Delta k},\ \zeta^2_{\Delta k} + a^2_{\Delta k}\eta^2_{k+\Delta k}\right). \quad (2)$$

In other words, the predicted albedo on the k-th day is $a_{\Delta k}\alpha^*_{k+\Delta k} + b_{\Delta k}$, and the corresponding prediction uncertainty consists in two components: the regression model

Discussion Paper | Discussion Paper | Discussion Paper | Discussion Paper |
HESSD
9, 9043–9064, 2012
Mapping spatially-temporally continuous shortwave albedo
N. Liu et al.
Title Page
Abstract Introduction
Conclusions References
Tables Figures
Back Close
Full Screen / Esc
Printer-friendly Version
Interactive Discussion

uncertainty $\zeta^2_{\Delta k}$ and the propagated observational uncertainty $a^2_{\Delta k}\,\eta^2_{k+\Delta k}$. Specifically, the PDF of α_k is $N\left(\alpha^*_k, \eta^2_k\right)$ when Δk equals to zero. Moreover, the PDF of α_k given its a priori multiyear mean μ_k and standard deviation σ_k is $N\left(\mu_k|\sigma^2_k\right)$ (see Sect. 3.2 for the calculation of μ_k and σ_k).

Assume the PDFs $P\left(\alpha_k|\alpha^*_{k+\Delta k}\right)$ ($\Delta k = -K, \ldots, K$) and $P\left(\alpha_k|\mu_k\right)$ are independent to each other. Then, given the surrounding GLASS02A2x observations $\alpha^*_{k+\Delta k}$ and the a priori multiyear mean μ_k, the joint PDF of α_k can be expressed as:

$$P\left(\alpha_k|\alpha^*_{k-K}, \ldots, \alpha^*_{k+K}, \mu_k\right) \sim N\left(\mu_k|\sigma^2_k\right) \prod_{\Delta k=-K}^{\Delta k=+K} N\left(a_{\Delta k}\,\alpha^*_{k+\Delta k} + b_{\Delta k},\, \zeta^2_{\Delta k} + a^2_{\Delta k}\,\eta^2_{k+\Delta k}\right). \quad (3)$$

Consequently, the maximum likelihood estimate of α_k takes the form:

$$\hat{\alpha}_k = \left(\frac{\mu_k}{\sigma^2_k} + \sum_{\Delta k=-K}^{\Delta k=+K} \frac{a_{\Delta k}\,\alpha^*_{k+\Delta k} + b_{k+\Delta k}}{\zeta^2_{\Delta k} + a^2_{\Delta k}\eta^2_{k+\Delta k}}\right) c \quad (4)$$

where c is the corresponding prediction variance:

$$c = 1 \Big/ \left(\frac{1}{\sigma^2_k} + \sum_{\Delta k=-K}^{\Delta k=+K} \frac{1}{\zeta^2_{\Delta k} + a^2_{\Delta k}\,\eta^2_{k+\Delta k}}\right). \quad (5)$$

Equations (4) and (5) are the statistics-based temporal filtering formula.

Equation (4) shows that the STF method, similar to the TSF algorithm proposed by Fang et al. (2007, 2008), is essentially a weighted average of statistical and observational values. Nevertheless, STF method has some advantages over the TSF methods. First, weights in the STF formula depend on both the temporal correlation and the observational errors of the albedos in neighboring days. In contrast, weights in TSF method are set to be an empirical function of temporal distance and take no account of observational errors. According to Eq. (4), observations with better correlation and less

HESSD
9, 9043–9064, 2012
Mapping spatially-temporally continuous shortwave albedo
N. Liu et al.

noise contribute more to the filtered result. Second, STF method can improve both the integrity and the smoothness of the GLASS02A2*x* albedo series. In the context of STF method, the observational albedo on the *k*-th day is smoothed if it is valid; or if not, the missing value is filled. Third, the a priori mean and standard deviation are employed to fill in data gaps in case of the absence of all surrounding observations. Finally, STF method provides an assessment of the uncertainty of filtered results.

3.2 The a priori knowledge database of global surface albedo

The a priori knowledge is of importance in retrieving BRDF/albedo parameters. For example, the retrievals of BDRF/albedo have been greatly improved owing to the adding of the a priori knowledge to the kernel-driven inversion model (Li et al., 2001). The back-up algorithm of MODIS BRDF/albedo products employs the prior BRDF shape information to address the limited angular sampling issue (Schaaf et al., 2002). In fact, both the regional climatology in ECF method and the multiyear average in TSF method are a form of prior information as well. In our study, the a priori statistics of global surface albedo are calculated from multiyear MCD43B3 products (from 2000–2010). There're several reasons for the utilization of MCD43B3 products: (1) great stability in its albedo time series and (2) great consistency between GLASS02A2*x* and MCD43B3 products (see Sect. 4.1). The a priori statistics are used to calculate the filter parameters ($a_{\Delta k}$, $b_{\Delta k}$ and $\zeta_{\Delta k}$), the a priori mean and standard deviation (μ_k and σ_k) in Eq. (4).

The a priori statistics derived from MCD43B3 products include: (1) multiyear albedo mean μ_k and standard deviation σ_k ($k = 1, 9, ..., 361$) and (2) correlation coefficient $\rho_{\Delta k}$ ($\Delta k = -32, -24, ..., 24, 32$) for the albedo in two neighboring days. Some regions, such as tropical areas covered by persistent cloud and polar areas affected by polar night, may miss multiyear statistical means. For polar areas, the average of statistical means on the two days before polar night is used to fill albedo mean gaps. For other regions, albedo means for each IGBP classification at each 10° latitudinal zone are calculated, and then used to replace statistical mean gaps according to their IGBP classification. In consideration of the storage consumption and the stability of the a priori statistics, the a priori knowledge dataset is at a 5-km spatial resolution and an 8-day temporal resolution.

To obtain the daily filter parameters and statistics required by Eq. (4), the 8-day a priori statistics need to be interpolated to a daily resolution and then converted to filter parameters. To this end, a polynomial interpolation technique is applied to statistical mean and standard deviation; and an exponential interpolation function is used for correlation coefficients. The curve fitting functions are as follows:

$$\begin{cases} \mu(\Delta d) = \lambda_1 \Delta d^3 + \lambda_2 \Delta d^2 + \lambda_3 \Delta d + \lambda_4 \\ \sigma(\Delta d) = \lambda_5 \Delta d^3 + \lambda_6 \Delta d^2 + \lambda_7 \Delta d + \lambda_8 \\ \rho(\Delta d) = \exp\left(\lambda_9 \Delta d^4 + \lambda_{10} \Delta d^2\right) \end{cases}. \tag{6}$$

Once the 8-day statistical mean, standard deviation and correlation coefficients are interpolated to a daily resolution, the daily statistics are converted to the filter parameters in Eq. (4):

$$\begin{cases} a_{\Delta k} = \rho_{\Delta k} \frac{\sigma_k}{\sigma_{k+\Delta k}} \\ b_{\Delta k} = \mu_k - a_{\Delta k} \mu_{k+\Delta k} \\ \zeta_{\Delta k} = \sqrt{\left(1 - \rho_{\Delta k}^2\right)} \sigma_k \end{cases}. \tag{7}$$

4 Result and analysis

4.1 Consistency between GLASS02A2*x* and MCD43B3 products

It should be noted that the inputs of STF algorithm are four kinds of GLASS02A2*x* albedo products derived from different algorithms and inputs. Great systematic discrepancy may appear among different GLASS02A2*x* products. Therefore, it is necessary to examine the consistency among the GLASS02A2*x* products before implementing

STF algorithm. Wide field measurements are the best way to examine the consistency between different products. However, such comprehensive datasets are inaccessible since the field observations usually cannot represent the pixel-level albedo. Therefore, to examine the consistency between different products by using a reference product is an alternative approach. The MODIS standard albedo product (MCD43B3), which is distributed by NASA since 2000, is the most widely used albedo products. It has a great stability and been widely validated and recognized. Therefore, it is employed to examine the consistency between GLASS02A2x products.

To avoid the influence of spatial and temporal discrepancies between different products, spatially-temporally homogeneous pixels are first selected from the 8-day GLASS02A0*x* and MCD43B3 products. For a pixel centered in a 3×3 spatial window on the k-th day, it is considered to be spatially-temporally homogeneous if:

1. all the pixels in 3×3 spatial window from day $(k-8)$ to day $(k+8)$ have the same land cover (see Table 3 for the classification criteria);

2. spatially relative differences between the albedo α_0 of center pixel and that of surrounding pixels α_i ($i = 1, 2, ..., 8$) are less than 5 %;

3. temporally relative differences between the spatially average on the k-th day and that on neighboring days are less than 5 %.

Once the spatially-temporally homogeneous pixels are selected, the statistics, including average, standard deviation, correlation coefficient, bias and root mean square error (RMSE), are computed at every 10° latitudinal zone. The statistical results provide some useful information about the consistency among albedo products (Table 4). First, the high correlation coefficients indicate a strong correlation between GLASS02A0*x* products and MCD43B3 product. Second, small biases and RMSEs indicate a good agreement between GLASS02A0*x* products and MCD43B3 product as well. Therefore, discrepancies among various GLASSABD2x products are considered to be negligible.

HESSD
9, 9043–9064, 2012

4.2 Results of STF algorithm

The STF technique was performed to post-process the global GLASS02A2*x* products and the resultant albedo dataset is named as GLASS02A06. Like GLASS preliminary albedo products, there's a quality assessment flag in GLASS02A06 product. Figure 2a and b are the comparison between GLASS02A21 and GLASS02A06 black-sky albedo of tile H25V05 in MODIS Sinusoid grid (from day 209–361, 2008, every 8 days). This area is located on the Tiber Plateau and is covered by water, grassland, bare soil and snow. It can be seen from Fig. 2a that, large number of data gaps (indicated by gray color) can be found in this area owing to cloud and seasonal snow coverage. After performing STF algorithm, the completeness of the GLASS preliminary albedo has been greatly improved. The spatial distribution of different land covers is well reflected in the GLASS02A06 albedo maps. Take the albedo map of day 209 as an example, bare soil areas are with red color, grasslands areas are with green color, small lakes are with dark blue color and residual snow areas are with yellow color. Seasonal variations in albedo are well depicted by the consecutive GLASS02A06 albedo maps. During day 209–241 (27 July–28 August), the albedo variability in this area was very small. During day 249–305 (5 September 31 October), the snow areas increased gradually with snowing process. During day 313–361 (8 November–26 December) snow areas decreased with smelting process.

The field albedo measurements at three automatic weather sites are selected to evaluate the performance of STF algorithm. These sites are BJ (31.3687° N/91.8987° E), D105 (33.0643° N/91.9426° E) and MS3478 (31.9262° N/91.7147° E) with a land cover of grassland. Figure 3 depicts the time series of field measurements, MODIS albedo (MCD43B3), GLASS preliminary (GLASS02A22) and final (GLASS02A06) albedo at these sites for year 2007. The a priori statistical mean and standard deviation series are also plotted in Fig. 3.

For all these sites, large statistical standard deviations are observed during the winter season. This may be associated with the surface heterogeneity caused by seasonal

HESSD
9, 9043–9064, 2012

snow. Seasonal variations or trends in albedo are well reflected by the series of statistical mean, field measurements, MODIS, GLASS preliminary and final albedo. During the non-winter season, the variations of surface albedo are very small. During the winter season, the surface albedo increases with snowing process and decreases with smelting process.

Compared to other series, the fluctuations of GLASS preliminary albedo series are much larger. This may result from the uncertainties of retrieving algorithm and the noise of input data. Besides, there are a lot of data gaps in GLASS preliminary albedo series because of the presence of cloud cover. After performing STF technique, the integrity and smoothness of GLASS preliminary albedo series are improved greatly. However, this should be interpreted with caution because some true fluctuations in albedo may be treated as noisy data as well. For instance, both the field measurements and GLASS preliminary results at MS3478 site show that there's an abrupt increase in surface albedo around day 141. However, this variation cannot be depicted in the GLASS final results since the STF method smoothes the GLASS preliminary series overly.

Generally, the GLASS final albedo series agrees well with the MODIS albedo series. However, the GLASS final results are more competent in capturing the variations in albedo. For instance, the field measurements indicate that a snowing and smelting process happened at BJ site from day 28 to day 41. GLASS final results captures this process well while it is missed by MODIS results. It may be associated with the retrieving method of MODIS albedo. In the context of MODIS method, reflectance of snow sometimes is abandoned to generate snow-free surface albedo. In winter, the field measurements decreased much faster than the GLASS final results. This may be attributed to the limited representation of field measurements. The field measurements cannot represent the pixel-level albedo which is retrieved by satellite data.

HESSD
9, 9043–9064, 2012

5 Conclusions

GLASS preliminary albedo products (GLASS02A2x, $x = 1$, 2, 3 and 4) are with high temporal resolution. Due to the factors such as cloud coverage, seasonal snow and other uncertainties, GLASS02A2x albedo products have large areas of missing data and sharp fluctuations.

Based on Bayesian theory, a statistics-based temporal filtering algorithm was proposed to fill in data gaps and smooth time series of GLASS02A2x products. The essence of STF method is a weighted average of the a priori statistics and albedo in neighboring days. Compared with other methods, this technique takes account of the statistical correlation and observational error and gives an assessment of the uncertainty of filtered results. The a priori statistics plays an important role in STF algorithm. When the number of valid preliminary albedo during the filtering temporal window is insufficient, the quality of filtered results is mostly determined by the a priori statistics. The current a priori database is calculated from 11 yr of MCD43B3 product. As new high-quality albedo product becomes available, the a priori database can be updated. However, the inter-annual change of the albedo statistics is not considered in this algorithm, which may bring some bias in trend change detection. On the other hand, the influence of the a priori database is negligible when there are enough valid GLASS preliminary albedo products. The uncertainty of STF result is indicated in the GLASS02A06 quality flag. It is recommended that the quality flag should always be checked when using the GLASS final albedo product.

Resultant albedo maps show that the STF method greatly improved the integrity of the final GLASS albedo product. Also, results at three automatic weather stations show that the smoothness of GLASS preliminary albedo products is improved by the STF method. Seasonal variations or trends in albedo are well depicted by the final GLASS albedo product. However, the STF method sometimes would smooth the GLASS preliminary albedo series overly. Compared with MODIS product, the final GLASS albedo product is much more competent in capturing the surface albedo variations.

HESSD
9, 9043–9064, 2012

Although it is an algorithm designed for GLASS albedo product, the STF algorithm is able to incorporate other albedo products, so long as the newly introduced product is statistically consistent with the current preliminary products (i.e. GLASS02A2*x*) and the a priori database which is derived from MCD43B3. It is also possible to apply the STF method to other parameters, such as the LAI and soil moisture, which presents a subject for our future study.

Acknowledgements. This work was financed by the National High Technology Research and Development Program of China (Grant No. 2009AA122100), National Natural Science Foundation of China (40901181, 91025006) and the EU Seventh Framework Program (CEOP-AEGIS). The author would like thank Nagqu Station of Plateau Climate and Environment and Cold and Arid Regions Environment and Engineering Research Institute, Chinese Academy of Sciences, for providing the field data at three automatic weather stations.

References

Barnes, C. A. and Roy, D. P.: Radiative forcing over the conterminous United States due to contemporary land cover land use albedo change, Geophys. Res. Lett., 35, L09706, doi:10.1029/2008gl033567, 2008.

Barnes, C. A. and Roy, D. P.: Radiative forcing over the conterminous United States due to contemporary land cover land use change and sensitivity to snow and interannual albedo variability, J. Geophys. Res., 115, G04033, doi:10.1029/2010jg001428, 2010.

Bsaibes, A., Courault, D., Baret, F., Weiss, M., Olioso, A., Jacob, F., Hagolle, O., Marloie, O., Bertrand, N., Desfond, V., and Kzemipour, F.: Albedo and LAI estimates from FORMOSAT-2 data for crop monitoring, Remote Sens. Environ., 113, 716-729, doi:10.1016/j.rse.2008.11.014, 2009.

Dickinson, R. E.: Land Surface Processes and Climate Surface Albedos and Energy-Balance, Adv. Geophys., 25, 305–353, 1983.

Dirmeyer, P. A. and Shukla, J.: Albedo as a modulator of climate response to tropical deforestation, J. Geophys. Res., 99, 20863–20877, doi:10.1029/94jd01311, 1994.

Fang, H., Liang, S., Kim, H.-Y., Townshend, J. R., Schaaf, C. L., Strahler, A. H., and Dickinson, R. E.: Developing a spatially continuous 1 km surface albedo data set over North America from Terra MODIS products, J. Geophys. Res., 112, D20206, doi:10.1029/2006jd008377, 2007.

Fang, H., Liang, S., Townshend, J. R., and Dickinson, R. E.: Spatially and temporally continuous LAI data sets based on an integrated filtering method: Examples from North America, Remote Sens. Environ., 112, 75–93, doi:10.1016/j.rse.2006.07.026, 2008.

GCOS: Systematic observation requirements for satellite-based products for climate-supplemental details to the satellite-based component of the implementation plan for the global observing system for climate in support of the UNFCCC, www.asic3.sdl.usu.edu/papers/gcos-unfccc.pdf (last access: July 2012), 2006.

Jin, Y. and Roy, D. P.: Fire-induced albedo change and its radiative forcing at the surface in northern Australia, Geophys. Res. Lett., 32, L13401, doi:10.1029/2005gl022822, 2005.

Ju, J., Roy, D. P., Shuai, Y., and Schaaf, C.: Development of an approach for generation of temporally complete daily nadir MODIS reflectance time series, Remote Sens. Environ., 114, 1–20, doi:10.1016/j.rse.2009.05.022, 2010.

Li, X., Gao, F., Wang, J., and Strahler, A.: A priori knowledge accumulation and its application to linear BRDF model inversion, J. Geophys. Res., 106, 11925–11935, doi:10.1029/2000jd900639, 2001.

Liang, S.: A direct algorithm for estimating land surface broadband albedos from MODIS imagery, IEEE T. Geosci. Remote, 41, 136–145, 2003.

Liang, S., Stroeve, J., and Box, J. E.: Mapping daily snow/ice shortwave broadband albedo from Moderate Resolution Imaging Spectroradiometer (MODIS): The improved direct retrieval algorithm and validation with Greenland in situ measurement, J. Geophys. Res., 110, D10109, doi:10.1029/2004jd005493, 2005.

Liang, S., Wang, K., Zhang, X., and Wild, M.: Review on Estimation of Land Surface Radiation and Energy Budgets From Ground Measurement, Remote Sensing and Model Simulations, IEEE J-Stars, 3, 225–240, 2010.

Liu, N., Liu, Q., Wang, L., and Wen, J.: A temporal filtering algorithm to reconstruct daily albedo series based on GLASS albedo product, Proceedings of International Geoscience and Remote Sensing Symposium (IGARSS), Vancouver, BC, 24–29 July 2011, 4277, 2011.

Manalo-Smith, N., Smith, G. L., Tiwari, S. N., and Staylor, W. F.: Analytic forms of bidirectional reflectance functions for application to Earth radiation budget studies, J. Geophys. Res., 103, 19733–19751, doi:10.1029/98jd00279, 1998.
Moody, E. G., King, M. D., Platnick, S., Schaaf, C. B., and Gao, F.: Spatially complete global spectral surface albedos: Value-added datasets derived from terra MODIS land products, IEEE T. Geosci. Remote, 43, 144–158, doi:10.1109/Tgrs.2004.838359, 2005.
Moritz, R. E., Bitz, C. M., and Steig, E. J.: Dynamics of Recent Climate Change in the Arctic, Science, 297, 1497–1502, doi:10.1126/science.1076522, 2002.
Qu, Y., Liu, Q., Liang, S., Wang, L., Liu, N., and Liu, S.: Direct-estimation algorithm for mapping daily land-surface broad band albedo from MODIS data, IEEE T. Geosci. Remote, in review, 2012.
Samain, O., Roujean, J.-L., and Geiger, B.: Use of a Kalman filter for the retrieval of surface BRDF coefficients with a time-evolving model based on the ECOCLIMAP land cover classification, Remote Sens. Environ., 112, 1337–1346, doi:10.1016/j.rse.2007.07.007, 2008.
Schaaf, C. B., Gao, F., Strahler, A. H., Lucht, W., Li, X., Tsang, T., Strugnell, N. C., Zhang, X., Jin, Y., Muller, J.-P., Lewis, P., Barnsley, M., Hobson, P., Disney, M., Roberts, G., Dunderdale, M., Doll, C., d'Entremont, R. P., Hu, B., Liang, S., Privette, J. L., and Roy, D.: First operational BRDF, albedo nadir reflectance products from MODIS, Remote Sens. Environ., 83, 135–148, doi:10.1016/s0034-4257(02)00091-3, 2002.

HESSD
9, 9043–9064, 2012

Mapping spatially-temporally continuous shortwave albedo

N. Liu et al.

Table 1. Yearly data gap percentage of MODIS MCD43B3 global shortwave black-sky albedo.

Year	2000	2001	2002	2003	2004	2005	2006	2007	2008	2009
Data gap Percentage (%)	32.72	37.60	28.57	22.86	21.90	21.81	21.91	22.39	23.56	23.56

HESSD
9, 9043–9064, 2012

Mapping spatially-temporally continuous shortwave albedo

N. Liu et al.

Table 2. Basic information of GLASS preliminary and intermediate albedo products.

Product	Rank	Algorithm	Source data	Spatial resolution	Temporal resolution	Composite length
GLASS02A21	Preliminary	AB1	MOD09GA	1 km	1 day	–
GLASS02A01	Mediate	Average	GLASS02A21	1 km	8 day	16 day
GLASS02A22	Preliminary	AB1	MYD09GA	1 km	1 day	–
GLASS02A02	Mediate	Average	GLASS02A22	1 km	8 day	16 day
GLASS02A23	Preliminary	AB2	MOD02A	1 km	1 day	–
GLASS02A03	Mediate	Average	GLASS02A23	1 km	8 day	16 day
GLASS02A24	Preliminary	AB2	MYD02A	1 km	1 day	–
GLASS02A04	Mediate	Average	GLASS02A24	1 km	8 day	16 day

HESSD
9, 9043–9064, 2012

Table 3. Classification criteria.

Criteria	Classification
$0.22 < \mathrm{NDVI}^{*} < 1$	Pure vegetation
$-1 < \mathrm{NDVI} < 0.15$ and $\alpha_{\mathrm{blue}} < 0.25$	Pure soil
$\alpha^{**}_{\mathrm{blue}} > 0.4$	Pure snow/ice
$0.15 < \mathrm{NDVI} < 0.22$	Vegetation + soil
$0.25 < \alpha_{\mathrm{blue}} < 0.4$	Snow/ice + soil

* Normalized difference vegetation index $\mathrm{NDVI} = \frac{\alpha_{\mathrm{NIR}} - \alpha_{\mathrm{Red}}}{\alpha_{\mathrm{NIR}} + \alpha_{\mathrm{Red}}}$, where α_{NIR} and α_{Red} are MCD43B3 albedo values at band1 and band2 respectively.

** α_{blue} is MCD43B3 albedo value at band3.

HESSD

9, 9043–9064, 2012

Mapping spatially-temporally continuous shortwave albedo

N. Liu et al.

Table 4. Statistical results of GLASS02A0x (x = 1, 2, 3 and 4) products.

Latitude	GLASS02A21			GLASS02A22			GLASS02A23			GLASS02A24		
band	ρ^{*}	b^{**}	ε^{***}	ρ	b	ε	ρ	b	ε	ρ	b	ε
70–80° N	0.995	−0.006	0.016	0.997	−0.003	0.016	0.994	−0.002	0.019	0.972	0.016	0.018
60–70° N	0.998	−0.002	0.016	0.996	0.001	0.016	0.999	−0.001	0.014	0.998	0.001	0.014
50–60° N	0.999	−0.006	0.016	0.998	0.001	0.017	0.999	0.002	0.013	0.999	0.004	0.013
40–50° N	0.999	−0.005	0.009	0.999	−0.001	0.009	0.998	0.002	0.007	0.999	0.004	0.007
30–40° N	0.988	0.012	0.008	0.990	0.009	0.008	0.994	0.015	0.008	0.992	0.014	0.007
20–30° N	0.989	0.002	0.008	0.995	0.020	0.005	0.992	0.009	0.007	0.987	−0.004	0.008
10–20° N	0.995	−0.007	0.007	0.995	−0.005	0.007	0.993	−0.002	0.009	0.993	−0.007	0.008
0–10° N	0.983	0.015	0.004	0.982	0.013	0.005	0.981	0.025	0.005	0.985	0.022	0.005
0–10° S	0.975	0.026	0.004	0.929	0.012	0.004	0.967	0.036	0.004	0.910	0.030	0.004
10–20° S	0.991	0.012	0.005	0.991	0.006	0.006	0.987	0.018	0.006	0.990	0.009	0.006
20–30° S	0.994	0.009	0.006	0.992	0.003	0.007	0.991	0.013	0.007	0.992	0.003	0.007
30–40° S	0.979	0.021	0.005	0.979	0.024	0.005	0.969	0.024	0.006	0.978	0.024	0.006

* ρ is the correlation coefficient between GLASS02A0x (x = 1, 2, 3 and 4) product and MCD43B3 product.
** b is the bias between GLASS02A0x (x = 1, 2, 3 and 4) product and MCD43B3 product.
*** ε is the regression root mean square error between GLASS02A0x andMCD43B3 product.

HESSD
9, 9043–9064, 2012

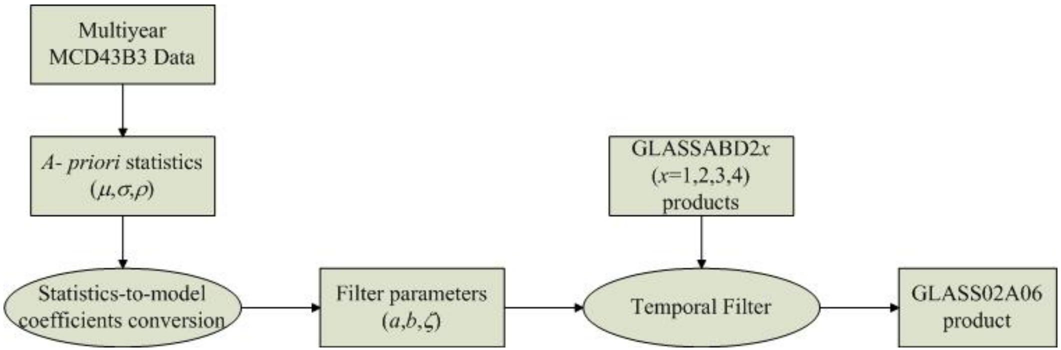

Fig. 1. Procedure of statistics-based temporal filtering algorithm.

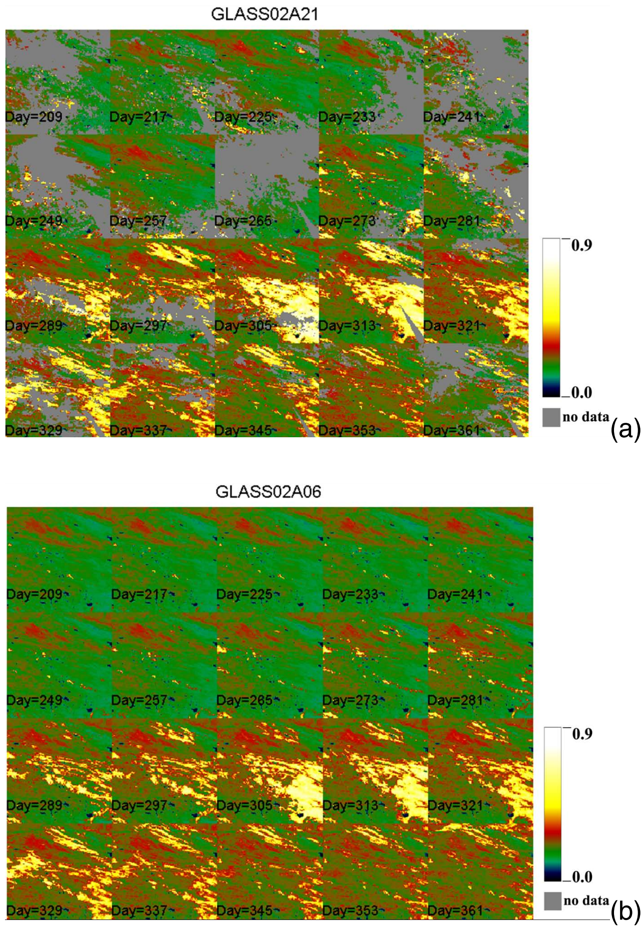

Fig. 2. Comparison of GLASS02A21 and GLASS02A06 albedo maps: **(a)** GLASS02A21 albedo maps and **(b)** GLASS02A06 albedo maps.

HESSD
9, 9043–9064, 2012

Mapping spatially-temporally continuous shortwave albedo

N. Liu et al.

Title Page
Abstract Introduction
Conclusions References
Tables Figures
Back Close
Full Screen / Esc
Printer-friendly Version
Interactive Discussion

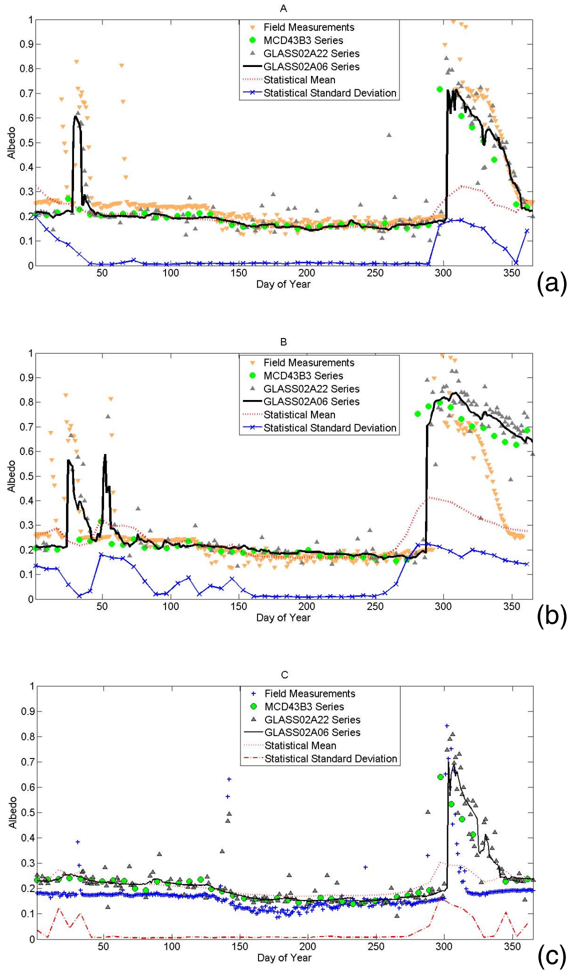

Fig. 3. Validation of STF methods at three automatic weather stations: **(a)** BJ (31.3687° N/91.8987° IE), **(b)** D105 (33.0643° N/91.9426° E) and **(c)** MS3478 (31.9262° N/91.7147° E).